

Scientific Article

High-Sulfated Hyaluronic Acid Ameliorates Radiation-Induced Intestinal Damage Without Blood Anticoagulation



Taichi Miura, PhD,^a Mitsuko Kawano, PhD,^a Keiko Takahashi, BS,^a
Noriyuki Yuasa, PhD,^b Masato Habu,^b Fumie Kimura, MS,^b
Toru Imamura, PhD,^{a,c} and Fumiaki Nakayama, MD, PhD^{a,*}

^aRegenerative Therapy Research Group, Department of Radiation Regulatory Science Research, National Institute of Radiological Sciences (NIRS), National Institutes for Quantum Science and Technology (QST), Chiba, Japan; ^bTokyo Chemical Industry Co, Ltd (TCI), Tokyo, Japan; ^cSchool of Bioscience and Biotechnology, Tokyo University of Technology, Hachioji, Japan

Received November 26, 2020; accepted January 13, 2022

Abstract

Purpose: Many growth factors, such as fibroblast growth factors (FGFs), are useful for the treatment or prevention of radiation damage after radiation therapy. Although heparin can be supplemented to increase the therapeutic effects of FGFs, it possesses strong anticoagulant effects, which limit its potential for clinical use. Therefore, chemically sulfated hyaluronic acid (HA) was developed as a safe alternative to heparin. This study examined the involvement of sulfated HA in radioprotective and anticoagulant effects.

Methods and Materials: FGF1 was administered intraperitoneally to BALB/c mice with sulfated HA 24 hours before or after total body irradiation with γ -rays. Several radioprotective effects were examined in the jejunum. The blood coagulation time in the presence of sulfated HA was measured using murine whole blood.

Results: FGF1 with high-sulfated HA (HA-HS) exhibited almost the same level of in vitro mitogenic activity as heparin, whereas FGF1 with HA or low-sulfated HA exhibited almost no mitogenic activity. Furthermore, HA-HS had high binding capability with FGF1. FGF1 with HA-HS significantly promoted crypt survival to the same level as heparin after total body irradiation and reduced radiation-induced apoptosis in crypt cells. Moreover, pretreatment of HA-HS without FGF1 also increased crypt survival and reduced apoptosis. Crypt survival with FGF1 in the presence of HA depended on the extent of sulfation of HA. Moreover, the blood anticoagulant effects of sulfated HA were weaker than those of heparin. As sulfated HA did not promote the reactivity of antithrombin III to thrombin, it did not increase anticoagulative effects to the same extent as heparin.

Conclusions: This study suggested that HA-HS promotes the radioprotective effects of FGF1 without anticoagulant effects. HA-HS has great potential for practical use to promote tissue regeneration after radiation damage.

© 2022 The Author(s). Published by Elsevier Inc. on behalf of American Society for Radiation Oncology. This is an open access article under the CC BY-NC-ND license (<http://creativecommons.org/licenses/by-nc-nd/4.0/>).

Sources of support: This study was supported by a grant for radiation emergency medical preparedness from the National Institutes for Quantum and Radiological Science and Technology.

Disclosures: Dr Miura, Dr Kawano, Ms Takahashi, Dr Yuasa, Mr Habu, and Dr Nakayama applied for patent 2019-145672 and PCT/JP2020/030349 issued to Tokyo Chemical Industry Co, Ltd, and National Institutes for Quantum and Radiological Science and Technology. Dr Miura, Dr Yuasa, and Mr Habu applied for patent 2018-30780 and PCT/JP2019/006806 issued to Tokyo Chemical Industry Co, Ltd, and Soka University. All other authors have no disclosures to declare.

All data generated and analyzed during this study are included in this published article.

*Corresponding author: Fumiaki Nakayama, MD, PhD; E-mail: nakayama.fumiaki@qst.go.jp

<https://doi.org/10.1016/j.adro.2022.100900>

2452-1094/© 2022 The Author(s). Published by Elsevier Inc. on behalf of American Society for Radiation Oncology. This is an open access article under the CC BY-NC-ND license (<http://creativecommons.org/licenses/by-nc-nd/4.0/>).

Introduction

Several fibroblast growth factors (FGFs), such as FGF1, FGF2, FGF7, and FGF10, have been reported to be effective in wound healing and in protecting against radiation-induced intestinal damage.^{1–10} In general, when these FGFs are used for wound healing or treatment of radiation-induced intestinal damage, they are frequently used in combination with exogenous glycans such as heparan sulfate and heparin (HP).⁹ Heparan sulfate is a member of the glycosaminoglycans (GAGs), which have a repeat of alternating uronic acid (glucuronid acid or iduronic acid) and *N*-acetylglucosamine (GlcNAc) units as their backbone. Sulfation of GAGs alters the properties of molecules by conferring a negative charge to regulate numerous physiological and pathologic events. In particular, heparan sulfate plays an important role in the stability of FGFs¹¹ and the binding of FGFs to FGF receptors (FGFRs) to increase FGF-FGFR signal transduction.¹² Other sulfated GAG chains also play roles in many biological processes, and a number of FGFs interact with these sulfated GAG subtypes.¹³

FGF1 protects against radiation-induced intestinal damage more effectively than other FGFs such as FGF2, FGF4, FGF7, and FGF10.⁶ However, the structural instability of FGF1 diminishes its potential for practical use.¹⁴ In contrast, HP has effects on wound healing and tissue repair¹⁵; therefore, it alone has potential as a radioprotector against radiation-induced oral mucositis.¹⁶ Moreover, the interaction with HP is able to stabilize FGF1 protein and extends its half-life^{7,9,11–14}; however, the addition of exogenous-free HP to FGFs may be pharmacologically difficult in clinical use due to its side effects. One of the most common side effects of HP is bleeding, which is caused by its strong anticoagulant effects.^{17,18} For this reason, the administration of HP to patients who are bleeding (eg, patients with thrombocytopenic purpura, vascular disorders, or hemophilia) or who are at risk of bleeding (eg, patients with visceral tumors, colitis, or severe hypertension) is prohibited or restricted.^{17,18} In addition, radiation-induced hemorrhage is an acute side effect that often develops in radiation therapy,^{19,20} and the administration of HP to patients with radiation-induced hemorrhage may also be difficult.

HP is used as an anticoagulant drug and a unique pentasaccharide sequence was identified as an antithrombin III (AT-III)–binding domain, which was responsible for the interaction with serine protease inhibitor AT-III, resulting in a conformational change and subsequent inhibition of major coagulation cascade proteases to exert its anticoagulant activity.²¹ The 3-*O*-sulfation of GlcNAc of this molecule produces the antithrombin-binding and antithrombotic activity.²¹

Heparan sulfate consists of a variably sulfated repeating sequence of uronic acid linked through an α -1,4-

glycosidic bond to GlcNAc, whereas hyaluronic acid (HA) is composed of a nonsulfated repeating sequence of uronic acid linked through a β -1,3-glycosidic bond to GlcNAc. Heparan sulfate and HA share a similar backbone structure except for sulfation; therefore, chemically sulfated HA may interact with a number of proteins, including FGFs, and may be used in physiological and pathologic events as a substitute for HP sulfate.^{1–8,11–13,22,23} For example, high-sulfated HA (HA-HS) interacts with FGF2 in medium and promotes FGF2 signaling in human-induced pluripotent stem cells.²² However, 3-*O*-sulfation of GlcNAc is impossible in HA because this position of GlcNAc is occupied by a β -1,3-glycosidic bond to GlcNAc, thus sulfated HA is not expected to have a strong effect on the inhibition of blood coagulation.^{21,22}

In this study, we found that HA-HS prevented radiation-induced intestinal damage in a mouse model of radiation injury. In addition, *in vitro* analysis revealed that the anticoagulant effects of HA-HS are weaker than those of HP.

Methods and Materials

Reagents

HP sodium salt (H3393) was purchased from Sigma-Aldrich (St. Louis, MO). HA, low-sulfated HA (HA-LS), and HA-HS were obtained from Tokyo Chemical Industry (Tokyo, Japan). His-tagged recombinant human FGF1 was purified as described previously.²⁴ Briefly, the human FGF1 gene was transferred into a pDEST17 vector (Invitrogen, Carlsbad, CA), which is an N-terminal fusion vector containing a sequence encoding a 6xHis tag. After the transformation of pDEST17 expression constructs into BL21(DE3)pLysS *Escherichia coli* cells, protein expression was induced using an Overnight Express Autoinduction System 1 according to the manufacturer's instructions (Novagen, Darmstadt, Germany). The cell pellet was lysed in BugBuster Master Mix (Novagen) containing an ethylenediaminetetraacetic acid–free cocktail (cComplete ULTRA; Roche Diagnostics, Mannheim, Germany), and soluble extracts were purified using Ni Sepharose High Performance columns (GE Healthcare, Little Chalfont Buckinghamshire, United Kingdom). Buffer exchange for recombinant proteins was performed by dialysis against phosphate-buffered saline.

Mice

Seven-week-old male BALB/c mice weighing 23 to 27 g were obtained from Clea Japan (Tokyo, Japan) and used in the present study. All mice were acclimated for 7 days. They were housed under specific pathogen-free conditions.

The animal rooms were maintained at 22°C to 24°C and 45% to 55% humidity with a 12:12-h light-dark schedule. Three to 5 mice were housed in aluminum cages with sterilized wood chips. The mice were provided with a pellet diet and chlorinated water (pH 2.8–3.0) was available ad libitum. The acidified water was used to prevent the spread of bacterial diseases in laboratory animals via drinking water. Eight-week-old mice were irradiated with a single dose of 4, 6, 10, or 12 Gy of whole-body γ -rays at a dose rate of approximately 0.43 Gy/min using a ^{137}Cs source (57.35 TBq, Gammacell 40; Atomic Energy of Canada, Ottawa, Canada). Mice were irradiated bilaterally in groups of up to 12 mice without anesthesia in an appropriate position using a cylindrical Plexiglas container (23 cm in diameter and 4 cm in height). The inside of the Plexiglas container was radially divided into 12 rooms by 3-mm thick walls and 1 mouse was placed per room. Doses were determined from the proportionality of irradiation time and dose relationship obtained from the radio-photoluminescence glass dosimeter Dose Ace GD-302M (AGC Techno Glass, Shizuoka, Japan). The radio-photoluminescence glass dosimeter was inserted into the center of the glass mouse phantom and values were converted into dose in Gy using the calibration constant, which was obtained from the ionization chamber (C-110, AE-132S; Applied Engineering Inc, Tokyo, Japan), which was calibrated to a national standard Co-60 source (111 TBq) at the National Institute of Advanced Industrial Science and Technology, Japan. The relationship between the dose absorbed in water Dw (Gy) at the center of the mouse phantom and the irradiation time X (sec) was expressed by the following equation: $Dw = 0.015 + 0.0086633 \times X$. The irradiation time was also calculated while correcting for attenuation using the attenuation correction factor of ^{137}Cs . The criteria for euthanasia were set at reaching a humane endpoint such as rapid mass weight loss or severe motor impairment. Peritoneal injection of sodium pentobarbital (Somnopentyl; Kyoritsu Seiyaku, Tokyo, Japan) at ~50 mg/kg body weight was used throughout the experiment for anesthesia. All protocols complied with the guidelines on animal experiments from the National Institute of Radiological Sciences (NIRS) and were approved by the Laboratory Animal Safety and Ethics Council of NIRS.

Cell growth assay

The murine interleukin 3-dependent pro B-cell line BaF3 was provided by RIKEN Bio Resource Center (Tsukuba, Japan). BaF3 cells express neither FGFR nor heparan sulfate proteoglycan.²⁵ The mitogenic response to FGF1 with HP, HA, or sulfated-HAs was examined using BaF3 transfectants overexpressing each FGFR, as described previously.²⁵ The proliferation of BaF3 transfectants using the tetrazolium salt WST-1 was assessed according to the manufacturer's protocol (Roche Diagnostics).⁶

Crypt assay

Ten micrograms of FGF1 together with 2.5 μg of HP, HA, HA-LS, or HA-HS was administered to mice 24 hours before or after total body irradiation (TBI) with γ -rays at 10 Gy. Crypt survival was examined 3.5 days after TBI to estimate the regeneration of the jejunum, as described previously.^{24,26,27} At 3.5 days after TBI with 10 Gy of γ -rays, 100% of the mice used in this study survived and none died or were euthanized before 3.5 days after TBI. In a previous report using the same irradiation device and the same Plexiglas container as those used in this study, the 50% lethal dose for BALB/c mice irradiated with 11.5 Gy of γ -rays was 6 days after TBI and no mice died at 3.5 days after TBI.⁸ Therefore, based on this previous result, mice were not expected to die within 3.5 days after TBI at doses below 11.5 Gy.⁸ At 3.5 days after TBI, approximately 11.2 to 14.0 cm of the mouse jejunum was removed, fixed in 10% buffered formalin, and embedded in paraffin. Paraffin sections, which were 3- μm thick and cut perpendicular to the long axis of the jejunum, were prepared for each mouse at 10 different portions of the jejunum. For each portion of the jejunum per mouse, 10 to 20 slices were prepared, and suitable slices for crypt measurement were selected and stained with hematoxylin (Sakura Finetek Japan, Tokyo, Japan) and eosin (Sakura Finetek Japan).²⁴ The number of surviving total crypts per circumference was counted on each paraffin-embedded cross-section from 10 portions of the jejunum using microscopy. Crypts were counted as viable if they contained more than 10 cells. The average number of crypts was divided by the average number in nonirradiated saline-treated control mice for normalization, and the normalized value is shown as the "crypt surviving fraction". In each group, 1 mouse was used for 1 experiment and 6 independent experiments were performed; therefore, the average number of surviving crypts for each group was obtained from 6 mice. The average number of surviving crypts per circumference of each jejunum cross-section in nonirradiated saline-treated control mice was approximately 130 and that in mice at 3.5 days after 10 Gy TBI was approximately 20 to 50. The number of surviving crypts after irradiation varied depending on the administration of FGF1 or GAGs.

TUNEL assay

Mice used for the terminal deoxynucleotidyl transferase-mediated 2'-deoxyuridine 5'-triphosphate nick end labeling (TUNEL) assay were intraperitoneally administered 2.5 μg of HP, HA, HA-LS, or HA-HS with or without 10 μg of FGF1 24 hours before TBI at 4, 6, or 12 Gy. The TUNEL assay was performed on paraffin-embedded sections of the jejunum to evaluate apoptosis 24 hours

after TBI at 4, 6, or 12 Gy.²⁸ Twenty-four hours after TBI, 3- μ m thick paraffin sections of the jejunum were prepared according to the same method as the crypt assay discussed previously. For each portion of the jejunum per mouse, 10 to 20 slices were prepared, suitable slices for the TUNEL assay were selected, and the assay was performed using an ApopTag Plus Peroxidase In Situ Apoptosis Detection Kit according to the manufacturer's protocol (Chemicon, Temecula, CA).²⁹ Briefly, tissue sections were deparaffinized and treated with 20 μ g/mL of Proteinase K and 3% H₂O₂ in phosphate-buffered saline. After equilibration with buffer, tissue sections were treated with a terminal deoxynucleotidyl transferase enzyme to label the 3'-OH ends of DNA fragments with digoxigenin nucleotides. Tissue sections were then incubated with a peroxidase-conjugated antidigoxigenin antibody at room temperature for 30 min and color development was performed using 3,3'-diaminobenzidine as a chromogen. After staining, at least 10 different portions in the jejunum of each mouse were photographed under a microscope at 20x magnification and the number of TUNEL + cells was assessed in 10 sequential cells in each crypt. The number of crypts per field was approximately 20 to 25, meaning that TUNEL + cells in approximately 200 to 250 crypts per mouse were measured in this study. The average number of TUNEL + cells/crypt in nonirradiated saline-treated control mice was approximately 0.24 ± 0.14 (data not shown). In each group, 1 mouse was used for 1 experiment and 4 independent experiments were performed; therefore, the average number of TUNEL + cells/crypt for each group was obtained from 4 mice.

Coagulation test

The blood coagulation time was measured by a modified method of the Lee-White test.³⁰ Heparin, HA, HA-LS, or HA-HS was added into each 2-mL polypropylene tube at a concentration of 1, 10, 100, or 1000 μ g/mL. One hundred microliters of whole blood from BALB/c mice was aliquoted into each tube and incubated at 37°C in a heat block. The first tube was tilted every 30 seconds until complete inversion caused no flow. All test tubes were then tilted until complete inversion caused no flow. The blood coagulation time was calculated to be the time when complete inversion caused no flow. The measurement was terminated when blood was not clotted after more than 3 hours. The same coagulation test was also performed using the whole blood from C57BL/6 mice.

Antithrombin assay

Antithrombin is the plasmatic inhibitor of thrombin, which can be greatly accelerated by HP. The influence of

sulfated HA on the antithrombin activity was assessed by indirect measurement of the antithrombin activity in plasma. Briefly, standard human plasma (lot number 503259A; Sysmex, Kobe, Japan) was reacted with an excess amount of thrombin reagent in the presence of sulfated HA. To estimate the residual thrombin in plasma, absorbance at 405 nm was measured after incubation with the chromogenic substrate using Berichrom Antithrombin III Auto B according to the manufacturer's instructions (Sysmex). In addition, the standard curve was made based on the reference measurement value of a dilution series of thrombin. The value of the sample was plotted on the standard curves to calculate the amount of residual thrombin, which correlated with the antithrombin activity in plasma.

Competitive enzyme-linked immunosorbent assay

Bovine serum albumin (BSA) (Sigma-Aldrich)-conjugated HP (BSA-HP) was prepared by the reductive amination method.³¹ Ninety-six-well plates were coated with BSA-HP by incubating wells with 2.5 μ g/mL solutions for 2 hours at room temperature. Wells were blocked with 1% BSA/tris-buffered saline with 0.1% tween 20 detergent (TBST) (pH 7.4). Recombinant human FGF1 (12.5 μ g/mL) was mixed with 10 μ g/mL of GAGs, such as HP, HA, HA-LS, and HA-HS, and these mixtures were incubated for 30 min at 4°C. These mixtures were then added to BSA-HP coated wells and incubated for 1 hour at 4°C. Unbound FGF1 was washed 3 times with 200 μ L of TBST. After washing, antihuman FGF1 antibody (Abcam, Cambridge, United Kingdom) was used as the primary antibody for detection. Wells were again washed and incubated with an horseradish peroxidase-conjugated antirabbit secondary antibody (Jackson Research Laboratories, PA). Wells were then washed and incubated with 100 μ L of tetramethylbenzidine solution (Surmodics, MN) for color development. Reactions were stopped with 1 N HCl and absorbance was measured at 450 nm. The ability of GAGs to bind to FGF1 is inversely related to the optical density (OD) value at 450 nm, that is, the lower the OD at 450 nm, the higher the binding ability of the GAG.²² Each average value of OD at 450 nm was obtained from 4 independent experiments.

Statistical analysis

All values represent the mean \pm standard deviation of results, and values in each group were compared using analysis of variance and Fisher's protected least significant difference test (* $P < .05$; ** $P < .01$; *** $P < .001$).

Results

HA-HS enhances the reactivity of FGF1 with FGFRs as well as HP

To examine the influence of sulfated HA on the *in vitro* mitogenic activity of FGF1, the proliferation of the BaF3 transfectants expressing FGFR1c, 2b, or 3c was measured after culturing with 100 ng/mL of FGF1 in the presence of HP, HA, HA-LS, or HA-HS at the indicated doses (Fig. 1A-C). The proliferation of BaF3-FGFRs increased at more than 0.005 or 0.05 $\mu\text{g/mL}$ of HP and peaked at 5 or 50 $\mu\text{g/mL}$ of HP. In contrast, HA-HS increased the proliferation of BaF3-FGFRs at more than 0.05 or 0.5 $\mu\text{g/mL}$ and it peaked at more than 50 $\mu\text{g/mL}$ of HA-HS. The mitogenic activity of FGF1 with HA-HS was less than 10-fold weaker than that with HP. However, HA-LS increased the proliferation of BaF3-FGFRs weakly and HA had no effect.

HP binds strongly to FGF1, stabilizing it and consequently promoting its signaling.^{9,11-14} Therefore, to examine the binding ability of sulfated HA to FGF1, we performed a competitive enzyme-linked immunosorbent assay (Fig. 1D). HA-HS bound to FGF1 as strongly as HP; however, the binding ability of HA-LS to FGF1 was weak and HA did not bind to FGF1.

Sulfated HA promotes the radioprotective effects of FGF1 and regeneration of the intestine after irradiation

GAGs, such as HP, may exert radioprotective effects because they can function as a co-receptor of FGFs, which are potential radioprotectors. Therefore, the radioprotective effects of HA-HS were evaluated by crypt assay. In a previous report, to investigate the radioprotective effects of HP and FGF1, the crypt assay was performed at 3.5 days after TBI with 8 to 12 Gy of γ -rays.⁸ The number

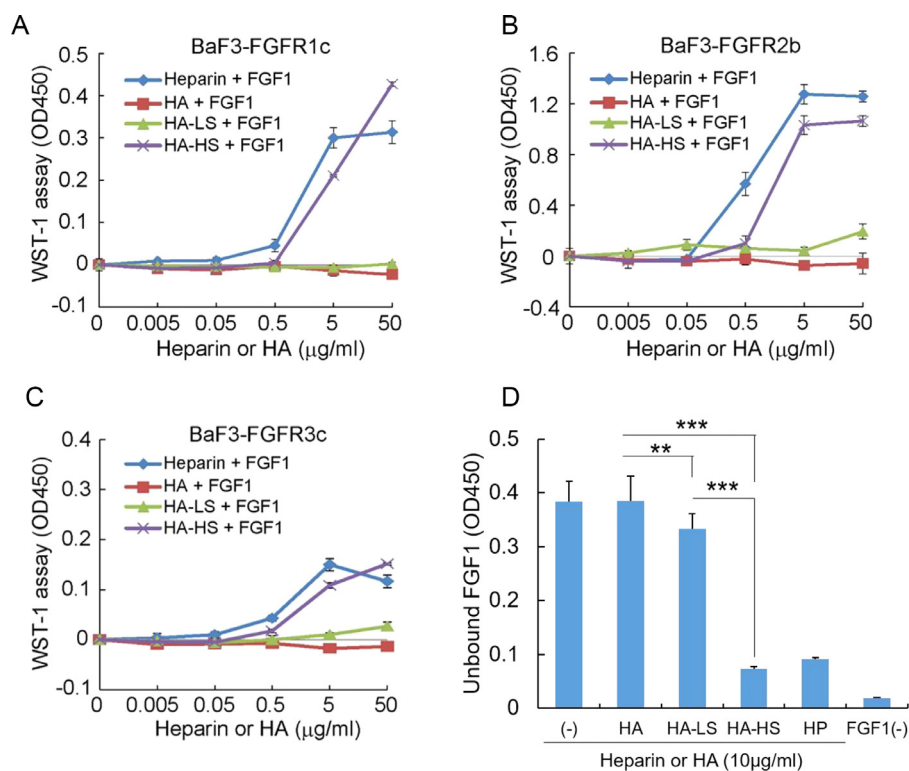


Fig. 1 High-sulfated hyaluronic acid (HA-HS) enhances the reactivity of fibroblast growth factor (FGF)1 with FGF receptors (FGFRs) as well as heparin (HP). BaF3 transfectant cell lines expressing FGFR1c (A), 2b (B), or 3c (C) were cultured for 42 hours in medium containing 100 ng/mL of FGF1 and the indicated concentrations of HP, HA, low-sulfated HA (HA-LS), or HA-HS. Cell numbers were estimated from optical absorbance at 450 nm (optical density [OD]450) using WST-1 reagent. A value of 0 on the horizontal axis corresponds to the condition where glycosaminoglycans (GAGs) were not added (only FGF1 was added). OD450 values of cells alone were almost 0, as were those of HA + FGF1 (data not shown). The values shown are the means \pm standard deviation (SD) of 6 independent experiments. (D) The binding activities of HA, HA-LS, HA-HS, and HP to FGF1 were measured by competitive enzyme-linked immunosorbent assay. As the residual amount of FGF1 not bound to GAGs was measured, OD450 was lower when the GAG had a higher ability to bind to FGF1. The values shown are the means \pm SD of 4 independent experiments.

of surviving crypts was large in control mice irradiated at doses below 8 Gy treated with saline, and no significant differences were noted in mice irradiated below 8 Gy treated with FGF1 and HP compared with controls.⁸ For these reasons, we performed the crypt assay after 10 Gy TBI in this study. Intraperitoneal pretreatment of 2.5 μ g of HA-HS into a mouse significantly promoted crypt regeneration after irradiation more than the saline pretreatment, but 25 μ g of HA-HS did not (Fig. 2A). Therefore, 2.5 μ g of each GAG was examined by crypt assay or TUNEL assay to estimate its radioprotective effects in the presence of FGF1.

To assess the therapeutic effects of sulfated HA on radiation damage in the intestine, these GAGs were administered alone or with FGF1 24 hours before or after TBI, and crypt survival was measured. Pretreatment with FGF1 increased crypt survival (Fig. 2B). In contrast, pretreatment with HP alone increased crypt survival to the same extent as that with FGF1 alone, and the combination of FGF1 and HP resulted in the greatest increase in crypt survival. On the other hand, pretreatment with HA-HS alone or in combination with FGF1 increased crypt survival to the same extent as that with HP alone or in combination with FGF1. However, the lethal dose_{50/6}, an index of gastrointestinal syndrome, was not increased by pretreatment with FGF1 in combination with HP or HA-HS in BALB/c mice (data not shown). HA also increased crypt survival, but the combination of HA and FGF1 had no effect. In contrast, HA-LS demonstrated almost the same pattern as HA-HS, but the combination of HA-LS and FGF1 did not significantly increase crypt survival compared with HA-LS alone. Therefore, among the GAGs tested, the intestinal radioprotective effects of HA-HS were most similar to those of HP.

Posttreatment with FGF1 alone increased crypt survival (Fig. 2C). In contrast, posttreatment with HP alone did not increase crypt survival, and the combination of HP and FGF1 significantly increased crypt survival compared with posttreatment with saline. Posttreatment with HA-LS or HA-HS alone significantly increased crypt survival compared with that with saline. However, there was no significant difference in crypt survival between FGF1 posttreatment together with HA-LS or HA-HS and posttreatment of HA-LS or HA-HS alone. In addition, posttreatment of HA was not as effective as that of HP or sulfated HA. This suggested that sulfated HA can promote crypt regeneration in the radiation-damaged intestine to the same degree as FGF1, but HP and HA have no such effect.

Sulfated HA inhibits radiation-induced apoptosis in the intestine

Previous reports demonstrated that FGF1 inhibits the apoptosis of crypt cells in mice irradiated with high doses

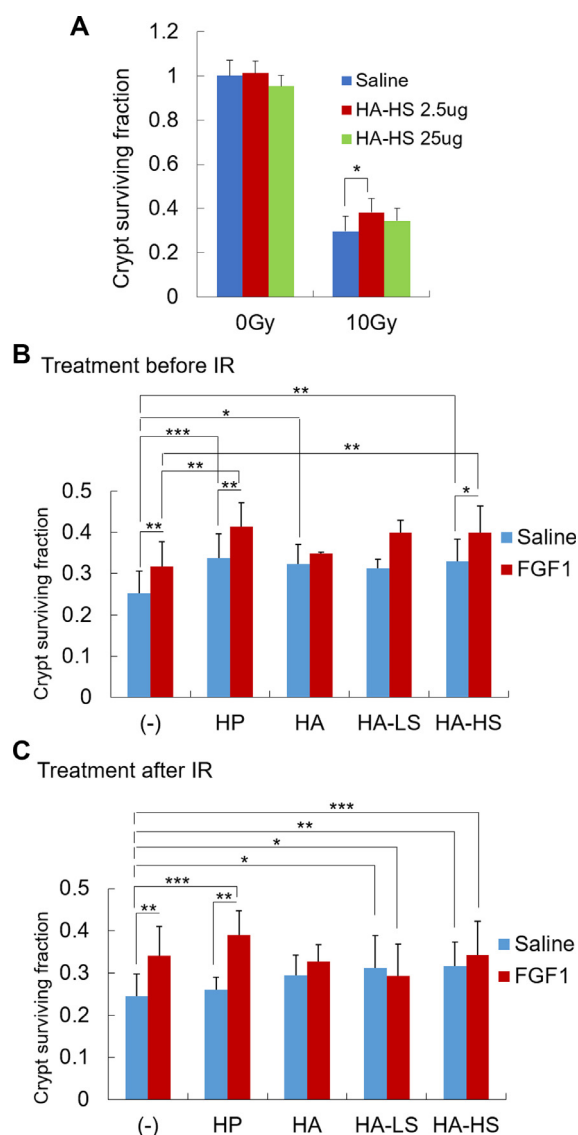


Fig. 2 Sulfated hyaluronic acid (HA) promotes the radioprotective effects of fibroblast growth factor (FGF)1 and regeneration of the intestine after irradiation. Ten micrograms of FGF1 was administered intraperitoneally to mice. The relative number of surviving crypts in the jejunum was measured 3.5 days after total body irradiation (TBI) with γ -rays at 10 Gy. (A) FGF1 with 2.5 or 25 μ g of high-sulfated HA (HA-HS) was administered to mice 24 hours before TBI. FGF1 together with 2.5 μ g of heparin (HP), HA, low-sulfated HA (HA-LS), or HA-HS was administered to mice 24 hours before (B) or after TBI (C). In each group, 1 mouse was used for 1 experiment and 6 independent experiments were performed. The values shown are the means \pm standard deviation of 6 independent experiments.

(12 Gy).⁶ Therefore, the TUNEL assay was performed to evaluate apoptosis 24 hours after 12 Gy irradiation (Fig. 3A, B). Pretreatment with FGF1 or HP alone reduced the number of TUNEL-positive cells. The

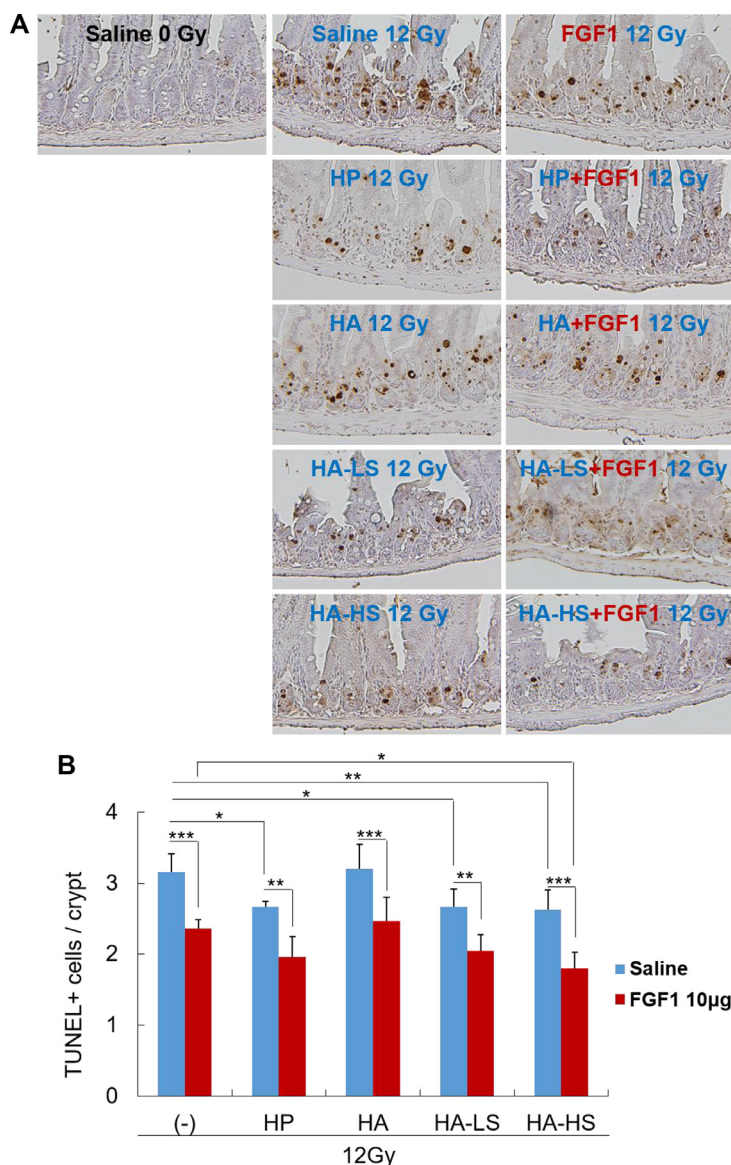


Fig. 3 Sulfated hyaluronic acid (HA) inhibits radiation-induced apoptosis in the intestine. Terminal deoxynucleotidyl transferase-mediated 2'-deoxyuridine 5'-triphosphate nick end labeling (TUNEL) assay was performed on paraffin-embedded sections of the jejunum to evaluate apoptosis 24 hours after total body irradiation (TBI) at 12 Gy. Mice used for TUNEL assay were intraperitoneally administered 2.5 µg of heparin (HP), HA, low-sulfated HA (HA-LS), or high-sulfated HA (HA-HS) with or without 10 µg of fibroblast growth factor (FGF)1 24 hours before total body irradiation (TBI) at 12 Gy. (A) The representative histologic images of the TUNEL assay are shown. (B) The number of TUNEL + cells was counted in each crypt 24 hours after irradiation. In each group, 1 mouse was used for 1 experiment and 4 independent experiments were performed. The values shown are the means ± standard deviation of 4 independent experiments.

combination of FGF1 and HP reduced the number of TUNEL-positive cells; however, there was no significant difference between the combination of FGF1 with HP and FGF1 alone. HA-HS and HP had similar antiapoptotic effects, and HA-LS exhibited almost the same antiapoptotic effects as HP, whereas HA had no antiapoptotic effects. In addition, HA-HS alone or with FGF1 significantly inhibited radiation-induced apoptosis after 4 or 6 Gy of TBI (Fig. E1). Therefore, sulfated HA itself inhibited radiation-induced apoptosis and HA-HS promoted the

inhibitory effects of FGF1 on radiation-induced apoptosis to a similar degree as HP.

Blood anticoagulant effects of sulfated HA are weaker than those of HP

If sulfated HA has anticoagulant effects like HP, it will be difficult to administer to patients with bleeding or a

risk of bleeding.^{17,18} Therefore, the blood coagulation time of sulfated HA was measured using murine whole blood (Fig. 4A). Low concentrations of HP had strong anticoagulant effects, whereas HA, HA-LS, and HA-HS had almost no anticoagulant effects at low concentrations (Fig. 4B). HP is clinically used at 10 $\mu\text{g}/\text{mL}$ when used as a blood anticoagulant, and this study confirmed that HP strongly inhibited blood coagulation for more than 3 hours at 10 $\mu\text{g}/\text{mL}$ (Fig. 4B, C). However, HA, HA-LS, and HA-HS, unlike HP, induced coagulation at 10 $\mu\text{g}/\text{mL}$ for less than 8 minutes (Fig. 4B, C). Therefore, the blood anticoagulant effects of HA-LS and HA-HS are weaker than those of HP. HA-HS promoted the reactivity of FGF1 to FGFRs to the same extent as HP at 5 $\mu\text{g}/\text{mL}$ (Fig. 1A-C) and increased the therapeutic effects of FGF1 at 2.5 $\mu\text{g}/\text{mL}$ (Fig. 2), suggesting that it activates the therapeutic effects of FGF1 with a lower risk of hemorrhage than HP.

Sulfated HA does not promote antithrombin activity in human plasma

AT-III is activated by the strong binding of HP to AT-III. Activated AT-III interacts with thrombin, a coagulation factor, and inhibits blood coagulation. Therefore, AT-III activity was evaluated by measuring the amount of residual thrombin after the addition of each GAG and thrombin to human plasma (Fig. 5). As HP promotes AT-III activity, the amount of residual thrombin decreased as the concentration of HP increased. In contrast, regardless of the concentration of HA or HA-LS, the amount of residual thrombin with HA or HA-LS was approximately 40% to 50% and was always higher than that with HP. The amount of residual thrombin with 1 to 100 $\mu\text{g}/\text{mL}$ of HA-HS was similar to that with HP, whereas that with 1000 $\mu\text{g}/\text{mL}$ of HA-HS was the highest of all conditions. Therefore, HA and sulfated HA, unlike HP, do not promote the reactivity of AT-III in human plasma to thrombin.

Discussion

Posttreatment of sulfated HAs promoted intestinal regeneration, but that of HP and HA did not. Thus, sulfated HA, especially HA-HS, unlike HP, may have radio-protective and regeneration-promoting effects in the small intestine, suggesting that the therapeutic effects of HA-HS were more useful than those of HP. Exogenous HA was suggested to increase the expression of endothelial growth factor, a signaling factor that promotes intestinal stem cell proliferation, and to increase crypt depth and villus height.³² Further studies are required to determine which signaling pathways, such as endothelial growth factor, are affected by sulfated HA in the mouse intestine.

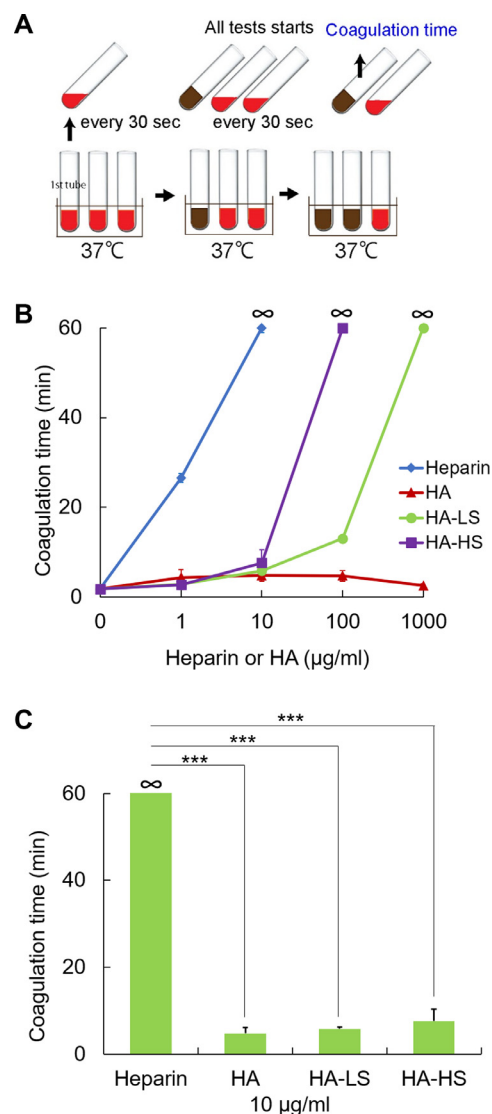


Fig. 4 Blood anticoagulant effects of sulfated hyaluronic acid (HA) are weaker than those of heparin. (A) The protocol for determining the blood coagulation time is shown. Whole blood from BALB/c mice was used for the coagulation test. The first tube was tilted every 30 s until complete inversion caused no flow. Then, each test tube was tilted every 30 s to determine the blood coagulation time. (B) The blood coagulation time was determined in the presence of heparin, HA, low-sulfated HA (HA-LS), or high-sulfated HA (HA-HS) at the indicated concentrations. The measurement was terminated when no blood clotting took place at more than 3 hours (∞). A value of 0 on the horizontal axis corresponds to the condition where glycosaminoglycans (GAGs) were not added (untreated condition). (C) The blood coagulation time was determined in the presence of 10 $\mu\text{g}/\text{mL}$ of heparin, HA, HA-LS, or HA-HS. Three independent coagulation tests were performed for each sample condition and the values shown are the means \pm standard deviation of the 3 independent tests. The same results were obtained in a coagulation test using whole blood from C57BL/6 mice (data not shown).

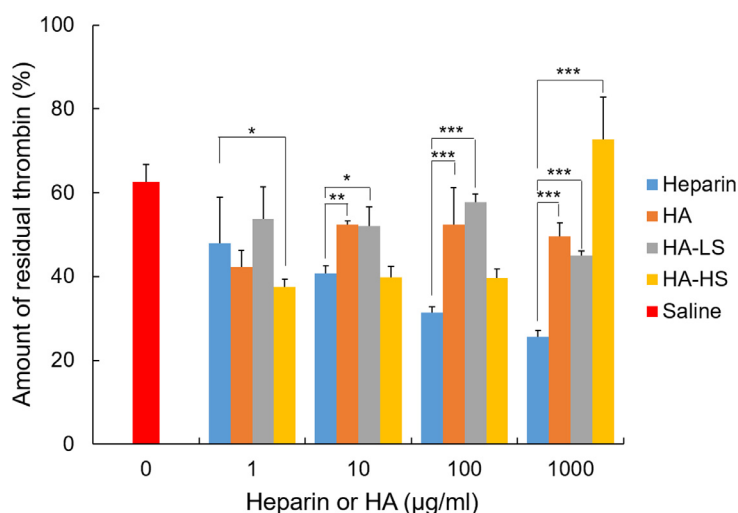


Fig. 5 Sulfated hyaluronic acid (HA) does not promote antithrombin activity in human plasma. For the antithrombin assay, commercially available standard human plasma was used. The activity of antithrombin III (AT-III) when the indicated concentrations of heparin, HA, low-sulfated HA (HA-LS), or high-sulfated HA (HA-HS) were added to human plasma was evaluated by measuring the amount of residual thrombin. "Saline" indicates the negative control without an added glycosaminoglycan (GAG). The values shown are the means \pm standard deviation of 3 independent experiments.

When the body is irradiated, reactive oxygen species (ROS), such as superoxide anion (O_2^-), hydroxyl radicals (OH^-), and hydrogen peroxide (H_2O_2), are generated, and these are toxic to nearby normal tissues.³³ This study did not examine whether HA-HS can scavenge these ROS. However, HP was previously reported to not scavenge O_2^- , OH^- , or H_2O_2 .³⁴ Therefore, HA-HS, which has a similar structure to HP, is also not expected to have scavenging activity for these ROS.

Compared with the treatment of HP, HA, HA-LS, or HA-HS alone before TBI, the combination of FGF1 and HP or HA-HS significantly increased crypt survival and their mean values were almost identical (Fig. 2B). In contrast, FGF1 combined with HA-LS slightly increased crypt survival, but this was not significantly different from HA-LS alone. The difference between the effects of HA-HS and HA-LS on FGF1 was due to HA-HS being more effective than HA-LS at promoting the reactivity of FGFRs and FGF1 (Fig. 1A-C). Furthermore, HA-HS, like HP, had high binding capability with FGF1, whereas HA-LS did not (Fig. 1D). Heparan sulfate and HP bind to both FGFs and FGFRs and promote FGF signaling by mediating complex formation between them.³⁵ Therefore, HA-HS may strongly bind both FGF1 and FGFRs, activating the downstream pathway of FGFRs and promoting the therapeutic effects of FGF1. Future analysis of the binding ability of HA-HS to FGFRs and identification of the downstream signaling pathway of FGFRs activated by the combination of HA-HS and FGF1 is needed.

FGF1 and FGF2 were reported to be effective in wound healing, and they are applicable to wound healing when combined with HP-based hydrogels.^{9,10} In addition, as HP binds to several wound-healing factors, such as vascular endothelial growth factor and transforming growth

factor β ,²³ combining these factors with HP-based hydrogels may enable more effective wound treatment. Therefore, the combination of HA-HS as a substitute for HP and different HP-binding factors, including FGFs, may be applied to treatments such as those for wound healing.

Our analyses demonstrated that sulfated HA did not promote the reactivity of AT-III to thrombin compared with HP (Fig. 5). HP also binds to coagulation inhibitors, such as HP cofactor II and protein C inhibitor, activating them and inhibiting coagulation in an AT-III-independent manner.³⁶ HA-HS at 10 $\mu\text{g}/\text{mL}$ did not inhibit coagulation, unlike HP, but the activity of AT-III on thrombin was comparable to that of HP (Figs. 4 and 5). This suggested that HA-HS inhibited the reactivity of AT-III to coagulation factors other than thrombin or inhibited coagulation inhibitors other than AT-III. Therefore, although our study provides evidence that HA-HS is an ideal HP alternative that avoids the risk of hemorrhage, the effects of HA-HS on the blood coagulation cascade require further analysis.

In the treatment of radiation-induced intestinal damage, HA-HS itself had therapeutic effects (Fig. 2B, C). Furthermore, the binding ability of HA-HS to FGF1 (data not shown) or FGF2²² was higher than that of GAGs other than HPs such as chondroitin sulfate, heparan sulfate, keratan sulfate, and dermatan sulfate. The efficacy of GAGs in multiple treatments has been evaluated, especially the therapeutic effects of high-sulfated chondroitin sulfate (CS) on dermatitis. High-sulfated CS has a high water-holding capacity and is used to treat skin inflammation. For example, high-sulfated CS was reported to be effective in the treatment of acute radiation dermatitis after breast radiation therapy.³⁷ HA-HS has not only a high water-holding capacity, but also a low risk of

hemorrhage and may activate signals involved in tissue repair, such as FGFs and vascular endothelial growth factor, to promote regenerative treatment effects. Therefore, HA-HS has great potential as an alternative to HP and is expected to have many future applications, including in the treatment of acute radiation dermatitis.

In the present study, the therapeutic effects of HA-HS were investigated using a mouse model of high-dose radiation injury, and its anticoagulant effects were examined by in vitro analysis. Therefore, further analysis using protocols similar to those used in human treatment, such as multiple rounds of radiation at low doses and partial abdominal irradiation, is necessary for the practical application of HA-HS. In addition, we irradiated mice with 10 and 12 Gy of γ -rays, but the dose irradiated to mice may vary depending on the condition and position of the mouse in the chamber during irradiation. Therefore, it is required to analyze not only with limited doses, such as 10 or 12 Gy, but also with other doses in the future. Moreover, in vivo analysis of the coagulation effects of HA-HS is also required for the practical application of HA-HS.

Conclusion

This study demonstrated that HA-HS, when administered alone or in combination with FGF1, protected against radiation-induced intestinal damage and promoted regeneration of the intestine after irradiation. Furthermore, we confirmed that HA-HS has weaker anticoagulant effects than HP. Therefore, HA-HS is an ideal HP substitute without the risk of hemorrhage and has great potential to be applied in the prevention and treatment of radiation-induced intestinal damage.

Acknowledgments

We express our gratitude to Ms. S. Umeda for technical assistance.

Supplementary materials

Supplementary material associated with this article can be found in the online version at [doi:10.1016/j.adro.2022.100900](https://doi.org/10.1016/j.adro.2022.100900).

References

- Khan WB, Shui C, Ning S, et al. Enhancement of murine intestinal stem cell survival after irradiation by keratinocyte growth factor. *Radiat Res.* 1997;148:248–253.
- Okunieff P, Mester M, Wang J, et al. In vivo radioprotective effects of angiogenic growth factors on the small bowel of C3H mice. *Radiat Res.* 1998;150:204–211.
- Takahama Y, Ochiya T, Tanooka H, et al. Adenovirus-mediated transfer of HST-1 / FGF-4 gene protects mice from lethal irradiation. *Oncogene.* 1999;18:5943–5947.
- Okunieff P, Li M, Liu W, et al. Keratinocyte growth factors radio-protect bowel and bone marrow but not KHT sarcoma. *Am J Clin Oncol-Canc.* 2001;24:491–495.
- Nakayama F, Hagiwara A, Kimura M, et al. Evaluation of radiation-induced hair follicle apoptosis in mice and the preventive effects of fibroblast growth factor-1. *Exp Dermatol.* 2009;18:889–892.
- Hagiwara A, Nakayama F, Motomura K, et al. Comparison of expression profiles of several fibroblast growth factor receptors in the mouse jejunum: Suggestive evidence for a differential radioprotective effect among major FGF family members and the potency of FGF1. *Radiat Res.* 2009;172:58–65.
- Nakayama F, Hagiwara A, Umeda S, et al. Post treatment with an FGF chimeric growth factor enhances epithelial cell proliferation to improve recovery from radiation-induced intestinal damage. *Int J Radiat Oncol.* 2010;78:860–867.
- Nakayama F, Umeda S, Yasuda T, et al. Structural stability of human fibroblast growth factor-1 is essential for protective effects against radiation-induced intestinal damage. *Int J Radiat Oncol.* 2013;85:477–483.
- Hui Q, Jin Z, Li X, et al. FGF family: From drug development to clinical application. *Int J Mol Sci.* 2018;19:1875.
- Wu J, Zhu J, He C, et al. Comparative study of heparin-polyoxamer hydrogel modified bFGF and aFGF for in vivo wound healing efficiency. *ACS Appl Mater Inter.* 2016;8:18710–18721.
- Gospodarowicz D, Cheng J. Heparin protects basic and acidic FGF from inactivation. *J Cell Physiol.* 1986;128:475–484.
- Yayon A, Klagsbrun M, Esko JD, et al. Cell surface, heparin-like molecules are required for binding of basic fibroblast growth factor to its high affinity receptor. *Cell.* 1991;64:841–848.
- Asada M, Shinomiya M, Suzuki M, et al. Glycosaminoglycan affinity of the complete fibroblast growth factor family. *Biochim Biophys Acta.* 2009;1790:40–48.
- Copeland RA, Ji H, Halfpenny AJ, et al. The structure of human acidic fibroblast growth factor and its interaction with heparin. *Arch Biochem Biophys.* 1991;289:53–61.
- Page C. Heparin and related drugs: Beyond anticoagulant activity. *ISRN Pharmacol.* 2013;2013: 910743.
- Kowaliuk M, Bozsaky E, Gruber S, et al. Systemic administration of heparin ameliorates radiation-induced oral mucositis-preclinical studies in mice. *Strahlenther Onkol.* 2018;194:686–692.
- Liang Y, Küick KL. Heparin-functionalized polymeric biomaterials in tissue engineering and drug delivery applications. *Acta Biomater.* 2014;10:1588–1600.
- Alban S. Adverse effects of heparin. *Hand Exp Pharmacol.* 2012;207:211–263.
- Kennedy AR, Maity A, Sanzari JK. A review of radiation-induced coagulopathy and new findings to support potential prevention strategies and treatments. *Radiat Res.* 2016;186:121–140.
- Hauer-Jensen M, Wang J, Denham JW. Bowel injury: Current and evolving management strategies. *Semin Radiat Oncol.* 2003; 13:357–371.
- Kusche M, Bäckström G, Riesenfeld J, et al. Biosynthesis of heparin. O-sulfation of the antithrombin-binding region. *J Biol Chem.* 1988;263:15474–15484.
- Miura T, Yuasa N, Ota H, et al. Highly sulfated hyaluronic acid maintains human induced pluripotent stem cells under feeder-free and bFGF-free conditions. *Biochem Biophys Res Co.* 2019;518:506–512.
- Olczyk P, Mencner Ł, Komosińska-Vashev K, et al. Diverse roles of heparan sulfate and heparin in wound repair. *Biomed Res Int.* 2015;2015: 549417.
- Nakayama F, Yasuda T, Umeda S, et al. Fibroblast growth factor-12 (FGF12) translocation into intestinal epithelial cells is dependent on a novel cell-penetrating peptide domain: Involvement of

- internalization in the in vivo role of exogenous FGF12. *J Biol Chem.* 2011;286:25823–25834.
25. Motomura K, Hagiwara A, Komi-Kuramochi A, et al. An FGF1: FGF2 chimeric growth factor exhibits universal FGF receptor specificity, enhanced stability and augmented activity useful for epithelial proliferation and radioprotection. *Biochim Biophys Acta.* 2008;1780:1432–1440.
 26. Withers HR, Elkind MM. Microcolony survival assay for cells of mouse intestinal mucosa exposed to radiation. *Int J Radiat Biol Relat Stud Phys Chem Med.* 1970;17:261–267.
 27. Nakayama F, Umeda S, Yasuda T, et al. Cellular internalization of fibroblast growth factor-12 exerts radioprotective effects on intestinal radiation damage independently of FGFR signaling. *Int J Radiat Oncol.* 2014;88:377–384.
 28. Miura T, Fujita M, Kawano M, et al. Strong radioprotective FGF1 signaling down-regulates proliferative and metastatic capabilities of the angiosarcoma cell line, ISOS-1, through the dual inhibition of EGFR and VEGFR pathways. *Clin Transl Radiat Oncol.* 2017;7:83–90.
 29. Gavrieli Y, Sherman Y, Ben-Sasson SA. Identification of programmed cell death in situ via specific labeling of nuclear DNA fragmentation. *J Cell Biol.* 1992;119:493–501.
 30. Sutton GC. Studies on blood coagulation and the effect of digitalis. *Circulation.* 1950;2:271–277.
 31. Gildersleeve JC, Oyelaran O, Simpson JT, et al. Improved procedure for direct coupling of carbohydrates to proteins via reductive amination. *Biocon Chem.* 2008;19:1485–1490.
 32. Riehl TE, Ee X, Stenson WF. Hyaluronic acid regulates normal intestinal and colonic growth in mice. *Am J Physiol-Gastr L.* 2012;303:G377–G388.
 33. Kim W, Lee S, Seo D, et al. Cellular stress responses in radiotherapy. *Cells.* 2019;8:1105.
 34. Lapenna D, Mezzetti A, de Gioia S, et al. Heparin: Does it act as an antioxidant in vivo? *Biochem Pharmacol.* 1992;44:188–191.
 35. Ornitz DN, Itoh N. Fibroblast growth factors. *Genome Biol.* 2001;2:REVIEWS3005.
 36. Mulloy B, Hogwood J, Gray E, et al. Pharmacology of heparin and related drugs. *Pharmacol Rev.* 2016;68:76–141.
 37. Sekiguchi K, Akahane K, Ogita M, et al. Efficacy of heparinoid moisturizer as a prophylactic agent for radiation dermatitis following radiotherapy after breast-conserving surgery: A randomized controlled trial. *Jpn J Clin Oncol.* 2018;48:450–457.